Integrated Torque Vectoring Control Using Vehicle Yaw Rate and Sideslip Angle for Improving Steering and Stability of All Off-Wheel-Motor Drive Electric Vehicles

Mahmoud Said Jneid, Péter Harth

Budapest University of Technologies and Economics, Department of Automotive Technologies, 1111 Budapest, Hungary
E-mails: mah.jneid@edu.bme.hu, harth.peter@kjk.bme.hu

Abstract: Recently electric vehicles with independent wheel-motor-drive showed great potential for advanced chassis active control integration leading to high driving performance, ensured safety, and compact packaging. Advanced motor drives and powerful power electronics enable highly sophisticated vehicle control systems to be applied and integrated using minimum hardware. This paper proposes an integrated torque vectoring control using vehicle yaw rate and sideslip angle to correct steering and improve stability of all off-wheel-motor drive electric vehicles. The control system is suggested with three control layers: the higher, medium, and lower. The main contribution of this work is implementing torque vectoring based on regenerative braking on the wheels allocated to develop braking force. The proposed torque vectoring control is implemented on a 7-DOF electric vehicle model in MATLAB/Simulink and verified by a double-lane change manoeuvre. Simulation results show explicit improvement in vehicle heading and stability.

Keywords: integrated torque vectoring; yaw rate; sideslip angle; electric vehicles; off-wheel-motor; regenerative braking; vehicle stability; steering correction

1   Introduction

Electric vehicles (EVs) have many advantages compared to conventional internal combustion engine (ICE) vehicles such as being environment-friendly, high efficiency, having a simple layout, minimized drivetrain elements, easy maintenance, improved packaging, and compactness. The present trends in the transportation sector suggest that EVs replace ICE vehicles shortly [1]. In all-wheel-motor drive (AWM) EVs, the electric motor can be installed inside the wheel so known as in-wheel-motor (IWM) or offside the wheel as is convented in this paper by off-wheel-motor (OWM). With four electric motors, the wheels' torque can be

precisely controlled allowing for the application of a wide range of advanced chassis assistance systems (ACAS) and advanced driver assistance systems (ADAS) as holistic integrated systems [2].

Thanks to electric motors and their sophisticated control algorithms, these systems can be implemented as an electronic version of the e-system achieving real drive-by-wire (DBW) and brake-by-wire (BBW) control [3], [4]. The e-system list includes an e-anti-lock braking system (eABS), an e-electronic stability program (eESP), an e-limited slip differential (eLSD), and e-torque vectoring (eTV) [5], [6]. Currently, TV is a hot research topic and attracts many researchers' attention and companies' interests working in the domain of electrified vehicles.

The principal behind the TV is to generate a corrective yaw moment around the vehicle's vertical axis to correct the vehicle heading during turning and cornering manoeuvres leading to improved vehicle stability and steering [7]. The precise torque control of electric motors (EMs) over a wide range of speeds in both traction and braking directions allows the generation of unlimited combinations of driving and braking differential force couples which can handle vehicle heading and stability under various conditions.

With TV, the vehicle behaviour is ensured linear if the desired yaw rate reference is generated according to the bicycle vehicle model. At some critical safety conditions such as severe understeering and oversteering, TV becomes indispensable in maintaining either neutral or acceptable understeering vehicle behaviour and hence stability level.

In understeering, the vehicle's front wheels reach the minimum limit of friction, thus, TV is expected to correct the vehicle heading by generation more yaw moment on the rear wheels in the direction of turning. Similarly, in oversteering, the rear wheels lose friction with the ground requiring the TV to produce a yaw moment acting opposite to the direction of overturning [8], [9].

In this paper, an integrated torque vectoring control (ITV) based on vehicle yaw rate and sideslip angle is proposed using a hysteresis controller to correct steering and improve stability of all off-wheel-motor drive electric vehicles. The control structure includes three layers: the high-level layer, the intermediate layer, and the lower layer. In the higher layer, the vehicle's yaw rate and sideslip angle control occur based on tracking the desired reference generated according to the bicycle model. In the intermediate layer, a coordination layer, where the corrective yaw moments of both yaw rate and sideslip angle are allocated to the individual wheels according to static load-based front-to-rear axle and equal-opposite of traction-braking couples as left-to-right distributions. Finally, in the lower layer, EMs control is implemented based on field-oriented control (FOC) to provide individually allocated torques.

The remainder of the article is structured as follows: Sec. 2 presents vehicle layout and subsystem models, Sec. 3 spotlights the proposed wheel slip-based integrated

vehicle yaw rate and sideslip angle TV control, Sec. 4 introduces results demonstration and investigation, and Sec. 5 concludes the work.

2 Vehicle Layout and Subsystem Models

To validate the proposed ITV control, a vehicle dynamic model (VDM) is developed in MATLAB/Simulink. The EV layout includes 4x EMs, 4x drive controllers, 4x reduction gears, 7-DOF VDM, driver, and battery models. The vehicle structure with power flow directions and control lines is best described in Fig. 1, which is reprinted from [2].
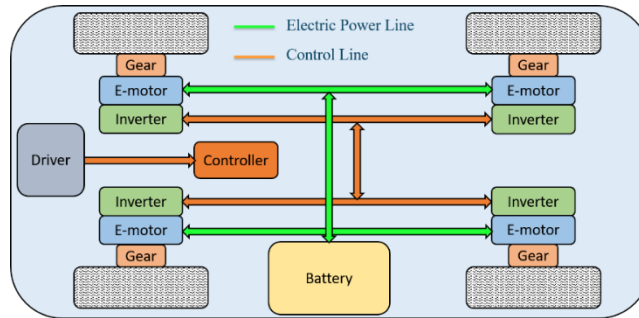

Figure 1

Schematic diagram of the suggested EV structure for the proposed ITV control

1.1 Vehicle Dynamic Model

For accurate validation of the proposed ITV control, the VDM is required to reflect the vehicle planar behaviour along with wheel dynamics precisely Therefore, a 7-DOF EV VDM is suggested to describe the longitudinal, lateral and yaw dynamics as well as the wheel's rotational dynamics as shown in Fig. 2. The equation of motion that describe the chassis planar behaviour is given in (1)-(2) as follows:

$$ma_x = F_f^x + F_r^x \tag{1}$$

$$ma_y = F_f^y + F_r^y \tag{2}$$

Where: m is the vehicle mass, a_x (a_y) vehicle's CoG longitudinal (lateral) acceleration, F_f^x (F_r^x) front (rear) longitudinal forces, F_f^y (F_r^y) front (rear) lateral forces. The vehicle yaw rate and sideslip angle are required for the ITV control integration and are given in (3)-(4) as follows:

$$I_z \dot{\gamma} = M_f^x + M_r^x + M_f^y + M_r^y \tag{3}$$

$$\beta = tan^{-1}\left(\frac{v_y}{v_x}\right) \tag{4}$$

With: $\dot{\gamma}$ vehicle's CoG yaw acceleration, I_z vehicle yaw moment of inertia, $M_f^x(M_r^x)$ front (rear) yaw moments resulting from longitudinal forces, $M_f^y(M_r^y)$ front (rear) yaw moments resulted from lateral forces, β vehicle sideslip angle, v_x (v_y) vehicle CoG longitudinal (lateral) speeds. Vehicle parameters are provided in Table 1.
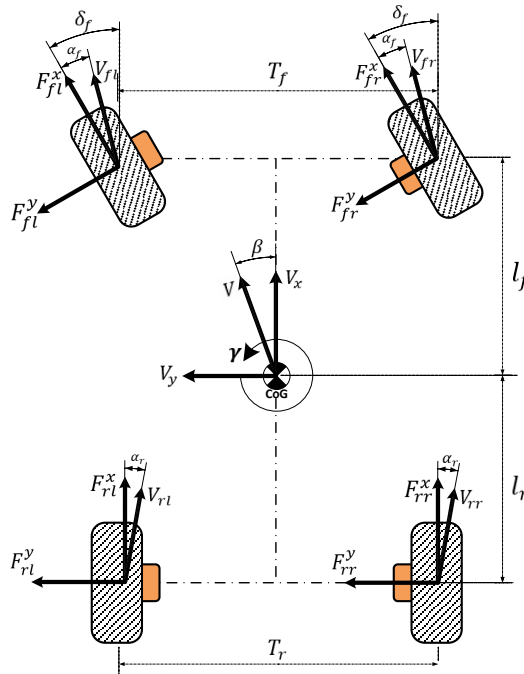

Figure 2

Schematic illustration of the 7-DoF VDM with wheels dynamic quantities

Table 1

Vehicle parameters

Parameter	Description	Value	Parameter	Description	Value
m	vehicle mass	1181kg	Lr	front axle distance from the centre of gravity	1.504 m
Af	vehicle frontal area	2.11 m2	Tf (Tr)	vehicle front (rear) track width	1.922 m
Cd	drag coefficient	0.33	h$_{CoG}$	vehicle centre of gravity height	0.134 m
Lf	rear axle distance from the centre of gravity	1.515 m	Iz	vehicle yaw inertia around the z-axis	2066 kg.m2

1.2   Tyre Model

Tires represent the interface of the vehicle to the external environment and are requested to be described with enough accuracy to reflect real vehicle behaviour. In literature, several tyre models are thoroughly investigated as describing real wheel dynamics for different purposes such as analysis, control, optimization, and simulation. The major models explored are the LuGre friction model [10], [11], the Dugoff model [12]-[14], the brush model [15]-[17], and Pacejka's magic formula (MF) model [18]-[20]. In this work, the MF model is chosen as it meets the performance requirements of combined dynamics and control of braking and traction forces under slip regulation at cornering necessary for performing the simulation of the double lane change (DLC) manoeuvre. MF model can be given according to (5), [21]:

$$y = Dsin[C\ tan^{-1}\{Bx - E(Bx - tan^{-1}(Bx))\}] \tag{5}$$

Where: y indicates the tyre output which can be either F_x or F_y, x represents wheel longitudinal or lateral slip κ or α. B, C, D, and E are empirical coefficients that denote the stiffness, shape, peak, and curvature of the MF solution, respectively. The tyre longitudinal slip κ under braking and traction conditions is given in (6):

$$\left. \begin{aligned} \kappa &= \frac{v_x - r_e \omega_w}{v_x} \\ \kappa &= \frac{r_e \omega_w - v_x}{r_e \omega_w} \end{aligned} \right\} \quad \begin{aligned} &at\ braking \\ \\ &at\ drivin \end{aligned} \tag{6}$$

The lateral slip or sideslip angle of the front and rear wheels are given in (7) as follows:

$$\begin{aligned} \alpha_f &= \beta + \frac{\gamma\ l_f}{v_x} - \delta \\ \alpha_r &= \beta - \frac{\gamma\ l_r}{v_x} \end{aligned} \tag{7}$$

The electrodynamic behaviour of wheels can be described according to Newton's second law as given in (8):

$$I_w\ \dot{\omega}_w = T_d - T_b - r_e\ F_x \tag{8}$$

Where: α_f (α_r) denotes the slip angle of the front (rear) wheels, γ the vehicle's yaw angle, δ wheel's steering angle, l_f (l_r) distance of the front (rear) axle to CoG, I_w the wheel's moment of inertia, $\dot{\omega}_w$ the wheel's angular velocity, T_d the electric motor wheel's driving torque, T_b the total braking torque from the EM and brakes, and r_e the wheel's effective radius.

Finally, the normal load of wheels in terms of static and dynamic weights are given according to (9) as follows [22]:

$$F_{fl}^z = \frac{m}{2(l_r+l_f)}\left(gl_r - h_{cg}a_x - \frac{2l_r h_{cg}}{T_f}a_y\right)$$

$$F_{fr}^z = \frac{m}{2(l_r+l_f)}\left(gl_r - h_{cg}a_x + \frac{2l_r h_{cg}}{T_f}a_y\right)$$

$$F_{rl}^z = \frac{m}{2(l_r+l_f)}\left(gl_r + h_{cg}a_x - \frac{2l_f h_{cg}}{T_r}a_y\right) \tag{9}$$

$$F_{rr}^z = \frac{m}{2(l_r+l_f)}\left(gl_r + h_{cg}a_x + \frac{2l_f h_{cg}}{T_r}a_y\right)$$

Where: F_{fl}^z (F_{fr}^z), F_{rl}^z (F_{rr}^z) indicate the weight on the front-left (front-right), and rear-left (rear-right) wheels respectively, g is the gravitational acceleration, and t_w is the vehicle's track width.

3   Integrated Torque Vectoring Control ITV

The main purpose of TV is to correct vehicle heading during cornering and maintain high stability through generating differential driving-braking forces which act at the vehicle's CoG to prevent undesired understeering and oversteering conditions. The differential forces from wheels result in a corrective yaw moment vector, which is generated by the main TV controller and has a direction the same as the vehicle turning.

Mainly, TV control consists of at least two control layers, the control and the distribution. The corrective yaw moment reference is generated in the control layer by tracking one or more parameters in terms of lateral stability. In-action states include the vehicle's yaw rate γ [2], [22]-[26], yaw rate γ and sideslip angle β [29]-[35], yaw rate γ and sideslip angle β with wheel slip κ [34]-[36]. Afterwards, the resulting yaw moment vector is broken into reference components based on allocation strategy and communicated to individual wheels' motor control. In literature, different TV control approaches investigated such as proportional-integral-differential (PID) [37], [38], neural network (NN) like PID [39], linear quadrature regulator (LQR) [40], [41], sliding mode control (SMC) [24], [42], [43], fuzzy logic control (FLC) [44], [45], FLC like PID [46], and model predictive control (MPC) [47]-[53].

In this work, a proposed integrated torque vectoring ITV control of the vehicle's yaw rate γ and sideslip angle β is implemented. The corrective yaw moment vector is distributed into the four wheels based on front-rear and right-left equal-opposite pairs of driving/braking components. Fig. 3 shows a block diagram of the proposed ITV control.
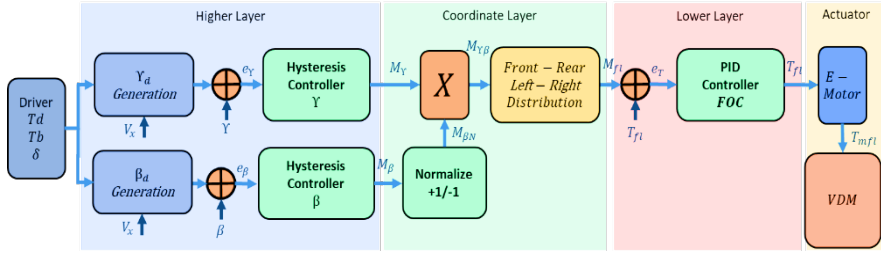
Figure 3

Block diagram of the proposed integrated torque vectoring control scheme ITV

3.1   Desired Control Reference

The ITV control is aimed at maintaining linear vehicle behaviour by tracking the vehicle's yaw rate γ and sideslip angle β. The desired reference values of γ and β can be derived based on the bicycle model with understeering behaviour k_u given in (10), (11) as follows [54]:

$$\gamma_d = \frac{v_x \, \delta}{(l_f + l_r) + k_u \, v_x{}^2} \tag{10}$$

$$\beta_d = \frac{l_r - l_f m \, v_x{}^2 / 2(l_f + l_r) C_f}{(l_f + l_r) + k_u \, v_x{}^2} \, \delta \tag{11}$$

With:

$$k_u = \frac{m}{(l_f + l_r)} \left(\frac{l_r}{C_f} - \frac{l_f}{C_r} \right) \tag{12}$$

Where: γ_d (β_d) denotes the desired yaw rate (sideslip angle), k_u understeering characteristic factor, C_f (C_r) the front (rear) wheel cornering stiffness according to [55].

3.2   Integrated Yaw Rate and Sideslip Angle Controller

In this work, the controller suggested for both γ and β is a hysteresis type. This controller meets the requirements of nonlinear control problems and is featured as a simple and model parameter-dependent controller. The output of γ controller is defined in (13) as follows:

$$M_\gamma = \left. \begin{array}{l} +K_\gamma \\ -K_\gamma \end{array} \right\} \begin{array}{l} if \ \ e_\gamma \geq \ 0 \\ if \ \ e_\gamma < \ 0 \end{array} \tag{13}$$

With:

$$K_\gamma = \frac{1}{I_z}(l_f C_f - l_r C_r)\beta + \frac{1}{v_x}(l_f{}^2 C_f - l_r{}^2 C_r)\gamma - l_f C_f \delta \tag{14}$$

The output of the β controller can be designated as follows:

At steady state, the side slip angle is very small [28], thus, (4) is simplified into (15):

$$\beta = \frac{v_y}{v_x} \tag{15}$$

With v_x constant, the derivative of (15) is given in (16):

$$\dot{\beta} = \frac{\dot{v}_y}{v_x} = \frac{a_y}{v_x} \tag{16}$$

Compensate (2) into (16) and fix it, the output of the β controller is assumed the $\dot{\beta}$ and defined in (17) as follows:

$$M_\beta = \left. \begin{matrix} +K_\beta \\ \\ -K_\beta \end{matrix} \right\} \begin{matrix} if\ \ e_\beta \geq\ 0 \\ \\ if\ \ e_\beta <\ 0 \end{matrix} \tag{17}$$

With:

$$K_\beta = \frac{1}{mv_x}(C_f + C_r)\beta + \frac{1}{v_y}\left((l_f C_f - l_r C_r)\right)\gamma - C_f \delta - m \tag{18}$$

Where: M_γ (M_β) is the corrective yaw moment vector generated by the yaw rate (sideslip angle) controller, e_γ (e_β) is the yaw rate (sideslip angle) error.

M_β is normalized between ±1 and used as a weight to bind the corrective yaw moment when the sideslip angle reaches the limit of stability that maintains vehicle safety. Eventually, the combined corrective yaw moment can be described in (19) as follows:

$$M_{\gamma\beta} = M_\gamma M_\beta \tag{19}$$

The resultant control law should be actuated by the four electric motors which represent an over-actuation control system. For optimal performance, $M_{\gamma\beta}$ is allocated according to the front-to-rear and right-to-left equal-opposite strategy. First, $M_{\gamma\beta}$ is distributed between the front and rear axles based on wheel static loads as in (20)-(22):

$$M_{\gamma\beta} = M_{\gamma\beta}^f + M_{\gamma\beta}^r \tag{20}$$

$$M_{\gamma\beta}^f = \frac{l_f}{l_f + l_r} M_{\gamma\beta}^f \tag{21}$$

$$M_{\gamma\beta}^r = \frac{l_r}{l_f + l_r} M_{\gamma\beta}^f \tag{22}$$

Afterwards, the front and rear yaw moment portions are distributed between the left and right wheels based on an equal-opposite combination according to (23)-(26):

$$M_{fl} = \left(\frac{1}{2}\right) M_{\gamma\beta}^{f} \, sign\,(\delta) \tag{23}$$

$$M_{fr} = -\left(\frac{1}{2}\right) M_{\gamma\beta}^{f} \, sign\,(\delta) \tag{24}$$

$$M_{rl} = \left(\frac{1}{2}\right) M_{\gamma\beta}^{r} \, sign\,(\delta) \tag{25}$$

$$M_{rr} = -\left(\frac{1}{2}\right) M_{\gamma\beta}^{r} \, sign\,(\delta) \tag{26}$$

Where: $M_{\gamma\beta}^{f}$ ($M_{\gamma\beta}^{r}$) is the front axle (rear axle) yaw moment portion, M_{fl} (M_{fr}) the yaw moment portion of the front-left (front-right), and M_{rl} (M_{rr}) the yaw moment portion of the rear-left (rear-right) wheels.

4   Simulation Results And Discussion

To validate the proposed ITV, a double lane change simulation manoeuvre (DLC) at 50kmh^{-1} speed is performed in MATLAB/Simulink. Results of ITV based on hysteresis controller are presented and compared to classical TV with PID controller (only yaw rate control) and when TV-off. Results are introduced in terms of the vehicle's and wheels' behaviours. The results discussion covers the vehicle's planer position, controlled yaw rater, controlled sideslip angle, lateral acceleration response, wheels' longitudinal (lateral) slip, modulated torques, speed, and energy recovery.

Fig. 4 shows the vehicle lateral position under the proposed ITV control, compared with yaw rate-based TV, and TV-off. A stable trajectory is confined with left and right cone boundaries at a distance of around 1.2 m from the vehicle centerline. With ITV control, the vehicle enters and exits the track at stable behaviour maintaining enough margins inside the lane. With conventional TV, the trajectory is maintained inside the borders slightly approaching the left cones at the manoeuvre egress. The worst case is when TV-off, where the vehicle bypasses the track boundaries during both lane changes indicating unstable behaviour.

Fig. 5 shows the vehicle yaw rate under ITV against TV behaviour and TV-off in response to the desired yaw rate. It can be seen that the ITV performs quite fast-tracking of the reference yaw rate with almost full matching. TV also behaves similarly with a slight overshoot in both lane changes noticeably at the point when the vehicle returns to the lane. However, when TV-off, the vehicle behaves more aggressively changing both lanes at a high yaw rate (far from the desired reference value with understeering characteristics) with a potential tendency to lose stability, especially at the end of the DLC manoeuvre where the vehicle performs excessive lane departure.

Fig. 6 demonstrates the vehicle sideslip angle of the ITV control compared with those of TV and TV-off. The realisation of sideslip angle control appears clearly in this figure, where the vehicle sideslip angle follows a confined and uniform course. In addition, it can be noticed that the sideslip angle under ITV and TV approach zero more quickly than that without control. This indicates vehicle stability is maintained, and the effectiveness of the proposed ITV control in correcting the vehicle's heading. However, with the TV-off, the vehicle is at the stability limit. In addition, the vehicle has no trajectory adjustment and is subject to loose controllability at severe manoeuvres, especially at the exit of the DLC test where the vehicle is assumed to return to its initial straight position more quickly.
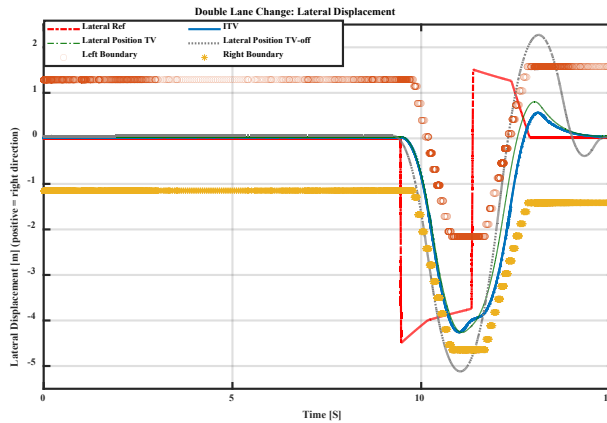

Figure 4

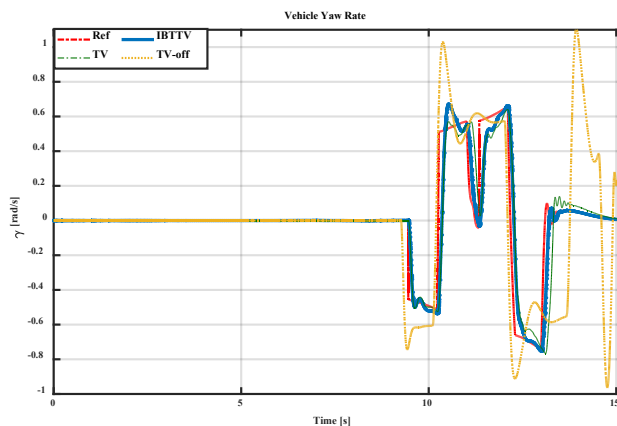Vehicle lateral displacement under ITV control compared to TV and TV-off

Figure 5

Vehicle yaw rate response under ITV control compared to TV and TV-off
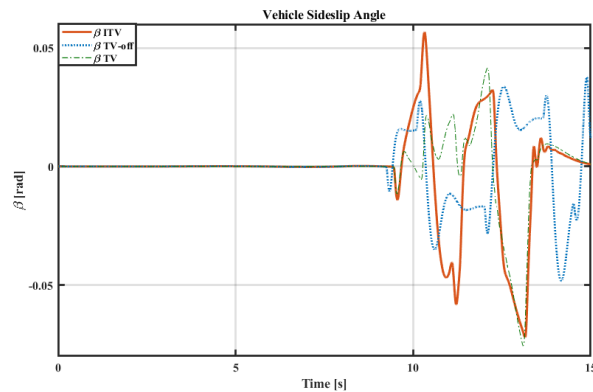
Figure 6
Vehicle sideslip angle under ITV control compared to TV and TV-off

Fig. 7 displays the vehicle lateral acceleration under ITV control, TV control, and TV-off. Again, stable vehicle behaviour can be the figure revealed with a max lateral acceleration of around 0.1 g, which is roughly lower than the max stability limit of 0.3 g. However, with TV-off, the vehicle quits the path at high acceleration with poor understeering characteristics.
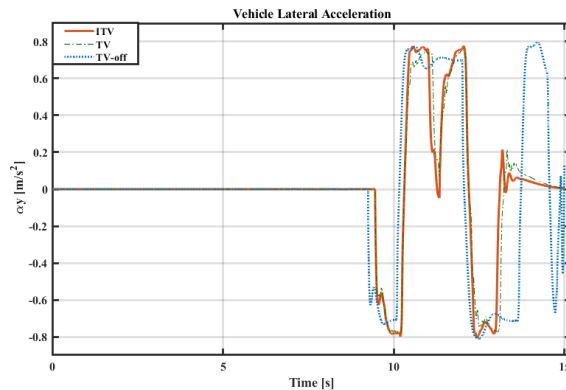

Figure 7
Vehicle lateral acceleration under ITV control compared to TV and TV-off

The potential performance of the ITV can be observed on the wheels' longitudinal slip as shown in Fig. 8. It is clear that the wheels' slip is maintained and limited within the optimal range [-0.2 to 0.2] for all front and rear wheels. This provides that the tyre-road friction is optimally utilised where wheels can generate max braking/traction forces. In contrast, wheels slip under both TV and TV-off exceeds the effective limit. To this end, the wheels under braking are subject to a locking-up case which may lead to vehicle stability issues, especially at lane change with high lateral acceleration.
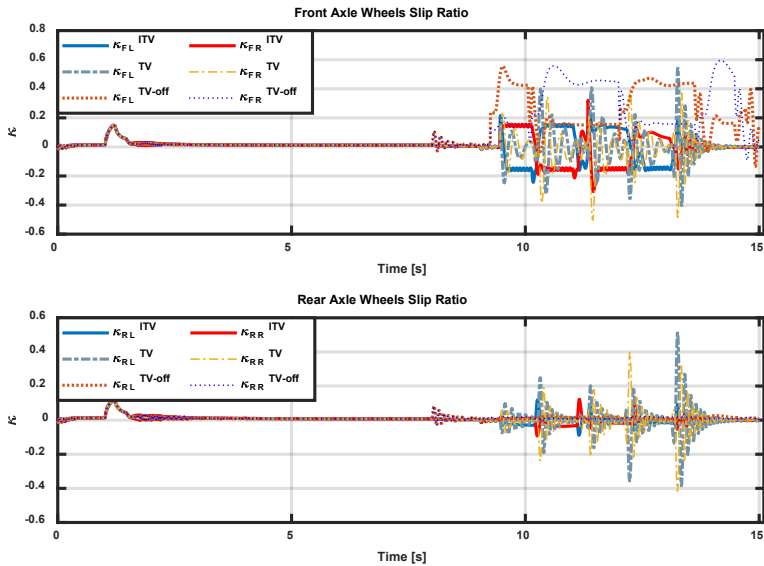
Figure 8
Wheels longitudinal slip under ITV control compared to TV and TV-off

Wheels slip angle regulation is a normal indirect consequence of the wheels' longitudinal slip regulation according to the fixed limit of the available friction circle. Fig. 9 demonstrates the slip angle of the front and rear wheels with stability control and without control. The slip angle of wheels under ITV and TV are confined within the range [-0.52 to 0.52], while it exceeds the range with TV-off. This is how the wheels slip angles and hence lateral forces are controlled indirectly when ITV is in action leading to maintaining vehicle lateral stability.

In response to ITV control, the wheels' torque and speed are adjusted according to the reference value from ITV as depicted in Figs. 10 and 11. It is clear that the wheels' dynamics are faster under the ITV than those of TV and TV-off. However, the fast wheels' behaviour can be attributed to the reality of the high dynamic ITV hysteresis controller. In contrast, the wheels' torque and speed with TV modified slightly, while they remained unchanged with TV-off as shown in the given figures.

The last part of this discussion is dedicated to battery conditions powering the electric motors. Fig. 12 presents the battery state of charge (SOC) under ITV control, TV control, and TV-off. It can be observed that the battery is less discharged with ITV SOC=90.5% compared to that of TV and TV-off. This can be attributed to the energy recuperation due to the regenerative braking of wheels allocated to generate a brake torque where brake current is used to recharge the battery. However, with TV, the battery is more discharged and SOC decreased to 88.25% without regenerative braking, while the highest energy consumption

occurred with TV-off at SOC 84.9% was observed as there is no brake component and wheels' torque or speed unmodulated.
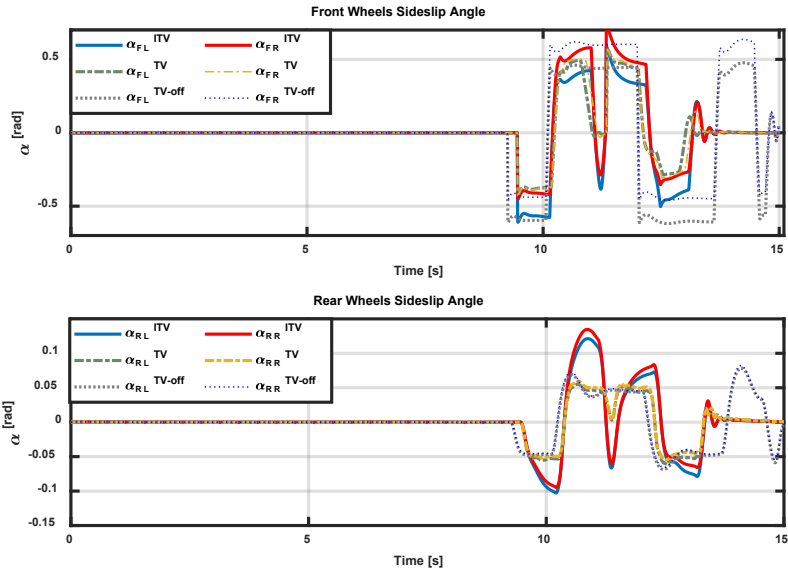
Figure 9

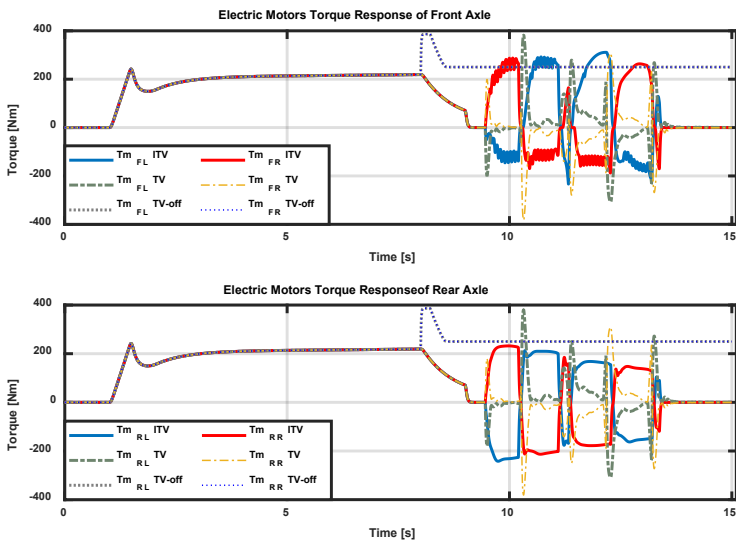Wheels slip angles under ITV control compared to TV and TV-off

Figure 10

Wheels adjusted torque under ITV control compared to TV and TV-off

Figure 11
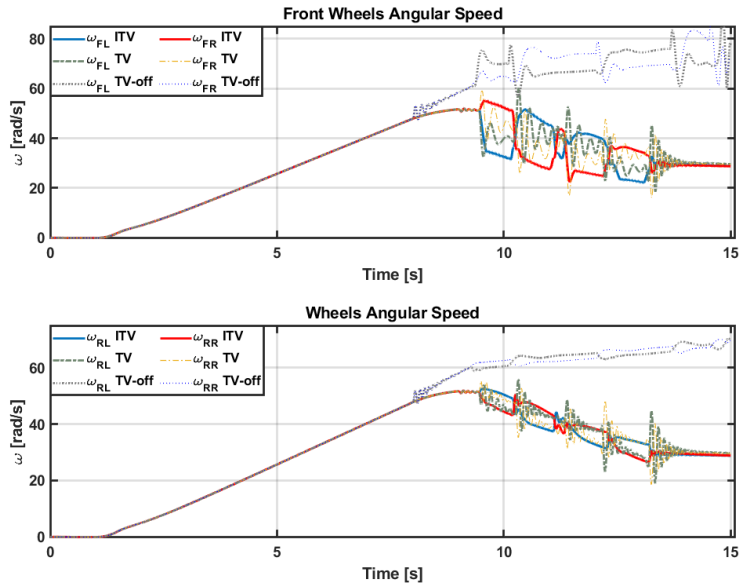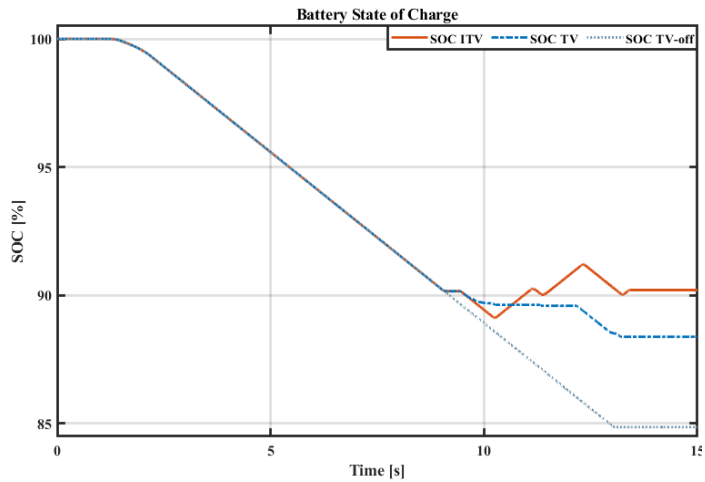Wheels adjusted velocity under ITV control compared to TV and TV-off

Figure 12
Battery SOC under ITV control compared to TV and TV-off

Conclusion

In this work, an integrated braking/driving torque vectoring (ITV) control is proposed based on yaw rate and sideslip angle tracking. The objective of the torque vectoring controller is to correct the vehicle heading during cornering by generating

two vectors of the corrective way moment and distributing the resultant yaw moment to the individual motors to maintain stability and improve vehicle handling. An axle load-based front-to-rear distribution and equal-opposite couples-based left-to-right distribution approaches are used for the yaw moment allocation.

A DLC simulation manoeuvre is performed on a 7-DOF electric vehicle model with AWD by OWM in MATLAB/Simulink to demonstrate the performance and effectiveness of the proposed IBTTV controller. Results reveal the effectiveness and the high performance of the proposed stability control in terms of vehicle stability, handling, and energy recovery.

The abbreviation list used in this work is provided in Table 2.

Table 2
Abbreviation list

Abbreviation	Description	Abbreviation	Description
ABS	Anti-Lock Braking System	FLC	Fuzzy Logic Control
ACAS	Advanced Chassis Assistance Active Safety	ICE	Internal Combustion Engine
ADAS	Advanced Driver Assistance System	ITV	Integrated Torque Vectoring
AWM	All-Wheel-Motor	IWM	In-Wheel-Motor
BBW	Brake-By-Wire	LQR	Linear Quadriture Regulator
CoG	Centre of Gravity	MF	Magic Formula
DLC	Double Lane Change	MPC	Model Predictive Control
DBW	Drive-By-Wire	NN	Neural Network
DOF	Degree of Freedom	OWM	Off-Wheel-Motor
eABS	e-Anti-Lock Braking System	PID	Proportional Integral Differential
eESP	e-Electronic Stability Program	SOC	State Of Charge
eLSD	e-Limited Slip Differential	SMC	Sliding Mode Control
EM	Electric Motor	TV	Torque Vectoring
EV	Electric Vehicle	VDM	Vehicle Dynamic Model
FOC	Field Oriented Control	FLC	Fuzzy Logic Control

References

[1]   M. Said Jneid, P. Harth, and P. Ficzere, "IN-WHEEL-MOTOR ELECTRIC VEHICLES AND THEIR ASSOCIATED DRIVETRAINS," *Int. J. TRAFFIC Transp. Eng.*, vol. 10, no. 4, Oct. 2020, doi: 10.7708/ijtte.2020.10(4).01

[2]   M. Said Jneid and P. Harth, "Integrated Braking and Traction Torque

Vectoring Control Based on Vehicle Yaw Rate for Stability Improvement of All-Wheel-Drive Electric Vehicles," *2023 IEEE Int. Conf. Electr. Syst. Aircraft, Railw. Sh. Propuls. Road Veh. Int. Transp. Electrif. Conf. (ESARS-ITEC), Venice, Italy*, no. Vdm, pp. 1–6, 2023, doi: 10.1109/ESARS-ITEC57127.2023.10114899

[3]   M. Said Jneid, M. Zöldy, and P. Harth, "Sensorless optimal control of electronic wedge brake based on dynamic model and Kalman filter state multiple-estimation," *Proc. Inst. Mech. Eng. Part D J. Automob. Eng.*, 2023, doi: 10.1177/09544070231168168

[4]   M. Said Jneid and A. Joukhadar, "LQR-Based Control of a Single Motor Electronic Wedge Brake EWB for Automotive Brake-By-Wire System," *Soft Comput. Electr. Eng.*, vol. 1, no. 1, pp. 12–35, 2019

[5]   M. Said Jneid and P. Harth, "Blended Regenerative Anti-Lock Braking System and Electronic Wedge Brake Coordinate Control Ensuring Maximal Energy Recovery and Stability of All-In-Wheel-Motor-Drive Electric Vehicles," *J. Transp. Technol.*, pp. 1–27, 2023

[6]   S. Woo, H. Cha, K. Yi, and S. Jang, "ACTIVE DIFFERENTIAL CONTROL FOR IMPROVED HANDLING PERFORMANCE OF FRONT-WHEEL-DRIVE HIGH-PERFORMANCE VEHICLES," *Int. J. Automot. Technol.*, vol. 22, no. 2, pp. 537–546, 2021, doi: 10.1007/s12239-021-0050-2

[7]   N. Ahmadian, A. Khosravi, and P. Sarhadi, "Integrated model reference adaptive control to coordinate active front steering and direct yaw moment control," *ISA Trans.*, vol. 106, pp. 85–96, Nov. 2020, doi: 10.1016/j.isatra.2020.06.020

[8]   A. Medina Murua, G. Bistue, A. Rubio, and J. Gonzalez, "A Direct Yaw Moment Control logic for an electric 2WD FSAE using an error cube PD controller."

[9]   L. De Novellis, A. Sorniotti, P. Gruber, and A. Pennycott, "Comparison of feedback control techniques for torque-vectoring control of fully electric vehicles," *IEEE Trans. Veh. Technol.*, vol. 63, no. 8, pp. 3612–3623, 2014, doi: 10.1109/TVT.2014.2305475

[10] Z. Li, P. Wang, H. Liu, Y. Hu, and H. Chen, "Coordinated longitudinal and lateral vehicle stability control based on the combined-slip tire model in the MPC framework," *Mech. Syst. Signal Process.*, vol. 161, Dec. 2021, doi: 10.1016/j.ymssp.2021.107947

[11] E. Hashemi, M. Pirani, A. Khajepour, and A. Kasaiezadeh, "A comprehensive study on the stability analysis of vehicle dynamics with pure/combined-slip tyre models," *Veh. Syst. Dyn.*, vol. 54, no. 12, pp. 1736–1761, Dec. 2016, doi: 10.1080/00423114.2016.1232417

[12] S. Rafatnia and M. Mirzaei, "Adaptive Estimation of Vehicle Velocity From Updated Dynamic Model for Control of Anti-Lock Braking System," *IEEE*

Trans. Intell. Transp. Syst., 2021, doi: 10.1109/TITS.2021.3060970

[13] M. A. Saeedi, "Simultaneous improvement of handling and lateral stability via a new robust control system," *Mech. Based Des. Struct. Mach.*, 2021, doi: 10.1080/15397734.2021.1888749

[14] M. Bian, L. Chen, Y. Luo, and K. Li, "A dynamic model for tire/road friction estimation under combined longitudinal/lateral slip situation," in *SAE Technical Papers*, 2014, vol. 1, doi: 10.4271/2014-01-0123

[15] A. O'Neill, J. Prins, J. F. Watts, and P. Gruber, "Enhancing brush tyre model accuracy through friction measurements," *Veh. Syst. Dyn.*, 2021, doi: 10.1080/00423114.2021.1893766

[16] K. B. Singh, M. A. Arat, and S. Taheri, "An intelligent tire based tire-road friction estimation technique and adaptive wheel slip controller for antilock brake system," *J. Dyn. Syst. Meas. Control. Trans. ASME*, vol. 135, no. 3, 2013, doi: 10.1115/1.4007704

[17] C. Ahn, H. Peng, and H. E. Tseng, "Robust estimation of road friction coefficient using lateral and longitudinal vehicle dynamics," in *Vehicle System Dynamics*, Jun. 2012, vol. 50, no. 6, pp. 961–985, doi: 10.1080/00423114.2012.659740

[18] S. Santini, N. Albarella, V. M. Arricale, R. Brancati, and A. Sakhnevych, "On-Board Road Friction Estimation Technique for Autonomous Driving Vehicle-Following Maneuvers," 2021, doi: 10.3390/app11052197

[19] K. B. Singh, "Vehicle sideslip angle estimation based on tire model adaptation," *Electron.*, vol. 8, no. 2, pp. 1–24, 2019, doi: 10.3390/electronics8020199

[20] C. W. Barson and K. J. Hardy, "Tyre and vehicle dynamics laboratory," *SAE Tech. Pap.*, 1989, doi: 10.4271/890107

[21] H. Pacejka, *Tire and Vehicle Dynamics*. 2012

[22] L. Su, Z. Wang, and C. Chen, "Torque vectoring control system for distributed drive electric bus under complicated driving conditions," *Assem. Autom.*, vol. 42, no. 1, pp. 1–18, Jan. 2022, doi: 10.1108/AA-12-2020-0194

[23] K. Y. J Y Park, S Na, H Cha, "Direct Yaw Moment Control With 4WD Torque-Vectoring For Vehicle Handling Stability And Agility," *Int.J Automot. Technol.*, vol. 23, pp. 555–565, 2022, [Online]. Available: https://link.springer.com/article/10.1007/s12239-022-0051-9

[24] G. Park, K. Han, K. Nam, H. Kim, and S. B. Choi, "Torque Vectoring Algorithm of Electronic-Four-Wheel Drive Vehicles for Enhancement of Cornering Performance," *IEEE Trans. Veh. Technol.*, vol. 69, no. 4, pp. 3668–3679, Mar. 2020, doi: 10.1109/tvt.2020.2978099

[25] Q. Lu, A. Sorniotti, P. Gruber, J. Theunissen, and J. De Smet, "H∞ loop

shaping for the torque-vectoring control of electric vehicles: Theoretical design and experimental assessment," *Mechatronics*, vol. 35, pp. 32–43, May 2016, doi: 10.1016/j.mechatronics.2015.12.005

[26] E. Morera-Torres, C. Ocampo-Martinez, and F. D. Bianchi, "Experimental Modelling and Optimal Torque Vectoring Control for 4WD Vehicles," *IEEE Trans. Veh. Technol.*, vol. 71, no. 5, pp. 4922–4932, 2022, doi: 10.1109/TVT.2022.3158091

[27] J. Liang *et al.*, "An Energy-oriented Torque-vector Control Framework for Distributed Drive Electric Vehicles," *IEEE Trans. Transp. Electrif.*, pp. 1–1, 2023, doi: 10.1109/tte.2022.3231933

[28] H. Wang, J. Han, and H. Zhang, "Lateral Stability Analysis of 4WID Electric Vehicle Based on Sliding Mode Control and Optimal Distribution Torque Strategy," *Actuators*, vol. 11, no. 9, 2022, doi: 10.3390/act11090244

[29] M. Vignati and E. Sabbioni, "A cooperative control strategy for yaw rate and sideslip angle control combining torque vectoring with rear wheel steering," *Veh. Syst. Dyn.*, vol. 60, no. 5, pp. 1668–1701, 2022, doi: 10.1080/00423114.2020.1869273

[30] R. Hajiloo, "Multi-Actuated Vehicle Control and Path Planning/Tracking at Handling Limits," 2021

[31] L. De Novellis, A. Sorniotti, P. Gruber, L. Shead, V. Ivanov, and K. Hoepping, "EVS26 International Battery, Hybrid and Fuel Cell Electric Vehicle Symposium Torque Vectoring for Electric Vehicles with Individually Controlled Motors: State-of-the-Art and Future Developments."

[32] M. Dalboni *et al.*, "Nonlinear Model Predictive Control for Integrated Energy-Efficient Torque-Vectoring and Anti-Roll Moment Distribution," *IEEE/ASME Trans. Mechatronics*, vol. 26, no. 3, pp. 1212–1224, Jun. 2021, doi: 10.1109/TMECH.2021.3073476

[33] E. Katsuyama, M. Yamakado, and M. Abe, "A state-of-the-art review: toward a novel vehicle dynamics control concept taking the driveline of electric vehicles into account as promising control actuators," *Veh. Syst. Dyn.*, vol. 59, no. 7, pp. 976–1025, 2021, doi: 10.1080/00423114.2021.1916048

[34] J. Wang, S. Lv, N. Sun, S. Gao, W. Sun, and Z. Zhou, "Torque vectoring control of rwid electric vehicle for reducing driving-wheel slippage energy dissipation in cornering," *Energies*, vol. 14, no. 23, pp. 0–16, 2021, doi: 10.3390/en14238143

[35] J. Kim and H. Kim, "Electric vehicle yaw rate control using independent in-wheel motor," *Fourth Power Convers. Conf. PCC-NAGOYA 2007 - Conf. Proc.*, pp. 705–710, 2007, doi: 10.1109/PCCON.2007.373043

[36] M. Said Jneid, P. Harth, and Á. Török, "Coordinate Torque Vectoring

Control For Enhancing Handling and Stability of All-Wheel-Drive Electric Vehicles Through Wheel Slip Control Integration," *2023 IEEE Cogn. Mobil. Conf. (CogMob), Budapest, Hungary. Forthcomming.*, 2023

[37]   J. Antunes, C. Cardeira, and P. Oliveira, "Torque Vectoring for a Formula Student Prototype," in *Advances in Intelligent Systems and Computing*, 2018, vol. 694, pp. 422–433, doi: 10.1007/978-3-319-70836-2_35

[38]   B. Peng, H. Zhang, and P. Zhao, "Research on the Stability Control Strategy of Four-Wheel Independent Driving Electric Vehicle," *Engineering*, vol. 09, no. 03, pp. 338–350, 2017, doi: 10.4236/eng.2017.93018

[39]   G. Cong, J. Biao, and Z. Xin, "Research on Torque Control Strategy for Electric Vehicle with In-wheel Motor," in *IFAC-PapersOnLine*, Jan. 2018, vol. 51, no. 31, pp. 71–74, doi: 10.1016/j.ifacol.2018.10.014

[40]   J. Antunes, A. Antunes, P. Outeiro, C. Cardeira, and P. Oliveira, "Testing of a torque vectoring controller for a Formula Student prototype," *Rob. Auton. Syst.*, vol. 113, pp. 56–62, Mar. 2019, doi: 10.1016/j.robot.2018.12.010

[41]   B. Zhao, N. Xu, H. Chen, K. Guo, and Y. Huang, "Stability control of electric vehicles with in-wheel motors by considering tire slip energy," *Mech. Syst. Signal Process.*, vol. 118, pp. 340–359, Mar. 2019, doi: 10.1016/j.ymssp.2018.08.037

[42]   X. Li, N. Xu, K. Guo, and Y. Huang, "An adaptive SMC controller for EVs with four IWMs handling and stability enhancement based on a stability index," *Veh. Syst. Dyn.*, vol. 59, no. 10, pp. 1509–1532, Oct. 2021, doi: 10.1080/00423114.2020.1767795

[43]   W. Cao, Z. Liu, Y. Chang, and A. Szumanowski, "Direct Yaw-Moment Control of All-Wheel-Independent-Drive Electric Vehicles with Network-Induced Delays through Parameter-Dependent Fuzzy SMC Approach," *Math. Probl. Eng.*, vol. 2017, 2017, doi: 10.1155/2017/5170492

[44]   L. Chen *et al.*, "Lateral Stability Control of Four-Wheel-Drive Electric Vehicle Based on Coordinated Control of Torque Distribution and ESP Differential Braking," 2021, doi: 10.3390/act10060135

[45]   L. S. Sawaqed and I. H. Rabbaa, "Fuzzy Yaw Rate and Sideslip Angle Direct Yaw Moment Control for Student Electric Racing Vehicle with Independent Motors," *World Electr. Veh. J.*, vol. 13, no. 7, pp. 1–12, 2022, doi: 10.3390/wevj13070109

[46]   Y. Lu, J. Lu, J. W. Wu, and B. Guo, "Study on the stability of high-speed turning braking based on the hardware-in-the-loop test," *Teh. Vjesn.*, vol. 25, no. 1, pp. 210–215, 2018, doi: 10.17559/TV-20170720161424

[47]   H. Deng, Y. Zhao, A.-T. Nguyen, and C. Huang, "Fault-Tolerant Predictive Control With Deep-Reinforcement-Learning-Based Torque Distribution for Four In-Wheel Motor Drive Electric Vehicles," *IEEE/ASME Trans.*

Mechatronics, pp. 1–13, 2023, doi: 10.1109/tmech.2022.3233705

[48]   G. Wang, Y. Liu, S. Li, Y. Tian, N. Zhang, and G. Cui, "New Integrated Vehicle Stability Control of Active Front Steering and Electronic Stability Control Considering Tire Force Reserve Capability," *IEEE Trans. Veh. Technol.*, vol. 70, no. 3, pp. 2181–2195, Mar. 2021, doi: 10.1109/TVT.2021.3056560

[49]   L. Wei, X. Wang, L. Li, Z. Fan, R. Dou, and J. Lin, "T-S Fuzzy Model Predictive Control for Vehicle Yaw Stability in Nonlinear Region," *IEEE Trans. Veh. Technol.*, vol. 70, no. 8, pp. 7536–7546, Aug. 2021, doi: 10.1109/TVT.2021.3091809

[50]   C. Li, Y. Xie, G. Wang, X. Zeng, and H. Jing, "Lateral stability regulation of intelligent electric vehicle based on model predictive control," doi: 10.1108/JICV-03-2021-0005

[51]   Q. Wang, Y. Zhao, F. Lin, C. Zhang, and H. Deng, "Integrated control for distributed in-wheel motor drive electric vehicle based on states estimation and nonlinear MPC," *Proc. Inst. Mech. Eng. Part D J. Automob. Eng.*, 2021, doi: 10.1177/09544070211030444

[52]   M. Ataei, A. Khajepour, and S. Jeon, "Model Predictive Control for integrated lateral stability, traction/braking control, and rollover prevention of electric vehicles," *Veh. Syst. Dyn.*, vol. 58, no. 1, pp. 49–73, Jan. 2020, doi: 10.1080/00423114.2019.1585557

[53]   B. Huang, S. Wu, S. Huang, and X. Fu, "Lateral Stability Control of Four-Wheel Independent Drive Electric Vehicles Based on Model Predictive Control," *Math. Probl. Eng.*, vol. 2018, 2018, doi: 10.1155/2018/6080763

[54]   S. Ding, L. Liu, and W. X. Zheng, "Sliding Mode Direct Yaw-Moment Control Design for In-Wheel Electric Vehicles," *IEEE Trans. Ind. Electron.*, vol. 64, no. 8, pp. 6752–6762, Aug. 2017, doi: 10.1109/TIE.2017.2682024

[55]   K. Nam, "Application of novel lateral tire force sensors to vehicle parameter estimation of electric vehicles," *Sensors (Switzerland)*, Vol. 15, No. 11, pp. 28385–28401, Nov. 2015, doi: 10.3390/s151128385